Available online at www.sciencedirect.com
ScienceDirect
Journal of Hazardous Materials 150 (2008) 68–75
Journal of Hazardous Materials
www.elsevier.com/locate/jhazmat

Critical wind velocity for arresting upwind gas and smoke dispersion induced by near-wall fire in a road tunnel

L.H. Hu *, W. Peng, R. Huo

State Key Laboratory of Fire Science, University of Science and Technology of China Hefei, Anhui 230026, China

Received 19 January 2007; received in revised form 15 April 2007; accepted 16 April 2007
Available online 24 April 2007

Abstract

In case of a tunnel fire, toxic gas and smoke particles released are the most fatal contaminations. It is important to supply fresh air from the upwind side to provide a clean and safe environment upstream from the fire source for people evacuation. Thus, the critical longitudinal wind velocity for arresting fire induced upwind gas and smoke dispersion is a key criteria for tunnel safety design. Former studies and thus, the models built for estimating the critical wind velocity are all arbitrarily assuming that the fire takes place at the centre of the tunnel. However, in many real cases in road tunnels, the fire originates near the sidewall. The critical velocity of a near-wall fire should be different with that of a free-standing central fire due to their different plume entrainment process. Theoretical analysis and CFD simulation were performed in this paper to estimate the critical velocity for the fire near the sidewall. Results showed that when fire originates near the sidewall, it needs larger critical velocity to arrest the upwind gas and smoke dispersion than when fire at the centre. The ratio of critical velocity of a near-wall fire to that of a central fire was ideally estimated to be 1.26 by theoretical analysis. Results by CFD modelling showed that the ratio decreased with the increase of the fire size till near to unity. The ratio by CFD modelling was about 1.18 for a 500 kW small fire, being near to and a bit lower than the theoretically estimated value of 1.26. However, the former models, including those of Thomas (1958, 1968), Dangizer and Kenndey (1982), Oka and Atkinson (1995), Wu and Barker (2000) and Kunsch (1999, 2002), underestimated the critical velocity needed for a fire near the tunnel sidewall.

Keywords: Critical velocity; Plume; Gas; Smoke; Dispersion; Road tunnel; Near-wall fire; FDS

1. Introduction

Tunnel fire is a hot concern around the world due to big fire disasters occur in road or railway tunnels in recent years, such as in Mont-Blanc, France/Italy [1] and Tauern, Austria [2] in 1999; Kitzsteinhorn, Austria in 2000; Gotthard, Switzerland in 2001; Dague, Korea in 2003 [3]; and Frejus, France/Italy in 2005 [4]. The environment in the tunnel will be polluted by smoke particle and poisonous gases, such as carbon monoxide, produced by the fire. The smoke particles decrease the visibility range in the space resulting in that the people who cannot find their way out. Also, the toxic gases directly harm and kill the evacuee [5]. Longitudinal wind flow commonly exists in tunnels. Natural airflow is induced by buoyancy due to temperature difference between the two portals due to the tunnel slope. Longitudinal ventilation system commonly designed in tunnels also forces airflow to go through the tunnel [6–11].

In case of a tunnel fire, there is an interaction between the longitudinal wind flow and gas/smoke dispersion induced by the fire. When the wind velocity is too low, fire gas and smoke disperses in both the upstream and downstream directions. However, due to the long narrow characteristic of the tunnel structure, it is important to ensure the space at the upstream side of the fire being free of smoke and toxic gases in an emergency of fire. Fresh airflow should enter the tunnel from the upstream portal for supplying oxygen for the evacuee and helping the fire fighter to approach the fire source for suppression. Thus, the critical wind velocity for arresting fire induced upwind gas and smoke dispersion is a key criteria for tunnel safety design.

2. Critical velocity models

Currently, there are several different models for predicting the critical velocity. Most of them are based on Froude or

* Corresponding author. Tel.: +86 551 3606446; fax: +86 551 3601669.
E-mail address: hlh@ustc.edu.cn (L.H. Hu).

0304-3894/$ – see front matter © 2007 Elsevier B.V. All rights reserved.
doi:10.1016/j.jhazmat.2007.04.094

Nomenclature

A	cross sectional area of the tunnel, (m^2);
C_1, C_2, C_3	constant in Kunsch's model;
C_p	specific heat capacity, ($J\,kg^{-1}\,K^{-1}$);
g	gravity acceleration constant, ($9.8\,m\,s^{-2}$);
H	tunnel height/height of computational domain, (m);
P	perimeter of the cross section of the tunnel, (m);
p	ambient pressure, (Pa);
Q	heat release rate of the fire, (kW);
Q^*	dimensionless heat release rate;
Q''	dimensionless heat release rate;
Ri	Richardson number;
T_0	ambient temperature, (K);
ΔT_0^*	dimensionless constant in Kunsch's model, 6.13;
U_c	critical wind velocity, ($m\,s^{-1}$);
U_c^*	dimensionless critical wind velocity;
$U_{c,c}$	critical velocity for central fire, ($m\,s^{-1}$);
$U_{c,w}$	critical velocity for near-wall fire, ($m\,s^{-1}$);
W	tunnel width;

Greek letters

ρ_0	ambient air density, ($kg\,m^{-3}$);
γ	ratio of specific heats of the fire gases;

Richardson modelling with assumption that there should be a balance between the energy of the incoming fresh air and that of the buoyant fire source at the critical condition [12]. These models have similar formation, including:

The Thomas model [13,14]:

$$U_c = \left(\frac{gHQ}{\rho_0 T_0 C_p A}\right)^{1/3} \tag{1}$$

The model proposed by Danziger and Kennedy [6]:

$$U_c = \left(\frac{gHQ}{\rho_0 T_0 C_p A Ri_c}\right)^{1/3} \tag{2}$$

with the critical Richardson number obtained to be 4.5 by Lee et al. [15] through scale model experiments.

The model proposed by Oka and Atkinson [7]:

$$U_c^* = 0.35\left(\frac{Q^*}{0.124}\right)^{1/3} \quad \text{for } Q^* < 0.124 \tag{3}$$

$$U_c^* = 0.35 \quad \text{for } Q^* > 0.124 \tag{4}$$

where $U_c^* = U_c/\sqrt{gH}$, $Q^* = Q/(\rho_0 C_p T_0 g^{1/2} H^{1/2} A)$

The model built by Wu and Barker [16]:

$$U_c' = 0.40\left(\frac{Q'}{0.20}\right)^{1/3} \quad \text{for } Q' \le 0.20 \tag{5}$$

$$U_c' = 0.40 \quad \text{for } Q' > 0.20 \tag{6}$$

where $U_c^* = U_c/\sqrt{g\bar{H}}$, $Q^* = Q/(\rho_0 C_p T_0 g^{1/2} \bar{H}^{5/2})$ with hydraulic diameter, $\bar{H} = 4A/P$, introduced into the model instead of the tunnel height, H. The models brought forward by Oka, Wu and Barker both take into account the 'super-critical wind velocity' which the critical wind velocity does not increase with one-third power of the heat release rate any more.

Recently, another simple model was brought forward by Kunsch [10,11] based on physical modelling of the plume rise and deflection at the tunnel ceiling. The critical velocity was related to the maximum plume temperature rise above the ambient, or the buoyancy force, when deflecting at the ceiling. This model seemed to investigate more deeply into the physics of the counteraction between the incoming fresh airflow and the buoyant plume gas driven by the fire, than the former models, which is considered roughly by the overall energy balance. The model built by Kunsch [11] is:

$$C_1 = \frac{1 - 0.1(H/W)}{1 + 0.1(H/2)}[1 + 0.1(H/W) - 0.015(H/W)^2] \cong 1 - 0.1(H/W) \tag{7}$$

$$C_2 = \frac{1 - 0.1(H/W)}{1 + 0.1(H/W)} 0.574(1 - 0.2(H/W)) \tag{8}$$

$$C_3 = 0.613 \tag{9}$$

$$U_c = C_3\sqrt{C_1 \Delta T_0^*}\frac{\sqrt{1 + (1 - C_2/C_1)\Delta T_0^* Q''^{2/3}}}{1 + \Delta T_0^* Q''^{2/3}} Q''^{1/3} \tag{10}$$

where ΔT_0^* is a dimensionless constant with value of 6.13 and $Q'' = Q/(\gamma/(\gamma - 1)p\sqrt{g}H^{5/2})$ with p to be the ambient pressure in Pa and γ to be the ratio of specific heats of the fire gases.

A comparison had been performed by Vauquelin [12] with his experimental results in a scale model tunnel. It was reported [12] that the model of Kunsch was close to the experimental value but still with an overestimation of about 10%. Also, the model of Thomas appeared to be in good agreement with experimental value for small fire sizes but with a small underestimation of the critical wind velocity. Although several different models are available, they all were verified only by scale model experiments or very little rough full scale experimental data, mainly because of the current lack of accurate full scale experimental data on critical velocity.

However, it should be noted that all the former studies and thus, the models built are all arbitrarily assuming that the fire takes place at the centre of the tunnel while in many real cases in a road tunnel, the fire originates near the sidewall. For example, fire is due to a collision to the sidewall or a burning vehicle is stopped by the driver at the emergency parking area, which is also near the wall in the road tunnel. For these near wall fires, the entrainment process of the fire plume and the development process of the deflected ceiling jet gas flow should be different from that of a fire freely standing at the tunnel centre. As shown in Fig. 1, the entrainment from the wall side is confined when the fire originates near the wall, while the freely standing fire plume entrainments fresh air from all around. With less

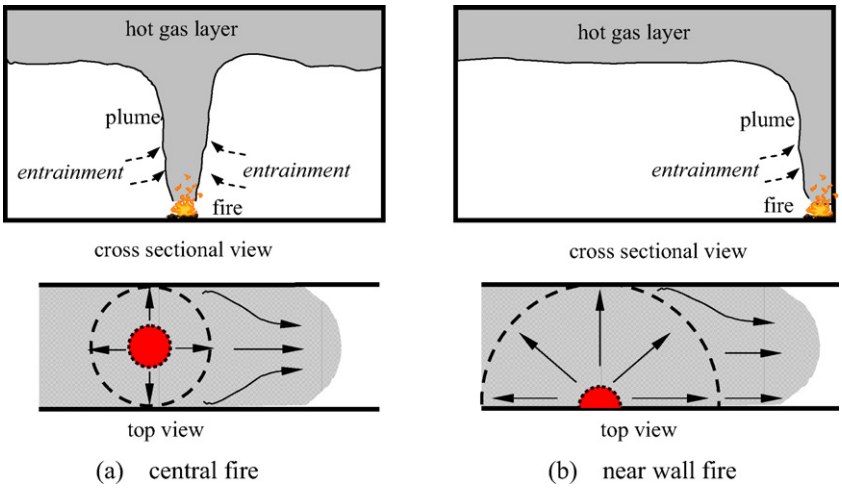

Fig. 1. Fire plumes for central fire and near wall fire in tunnels.

air mass entrained, the plume front has higher upward velocity and higher temperature [17] when deflecting at the ceiling. These two parameters are both key factors dominating the buoyancy force to drive the fire gas flow. So, the critical velocity for fire originated near the sidewall of the tunnel should be different with that of a freely standing case and should be further investigated.

3. Theoretical analysis

The interaction of fire plume with wall or corner in a compartment had been formerly studied [17,18]. A "mirror" effect was considered under these conditions. It was reported that the plume attached to the wall would develop as a half-plume with plume properties approximating those for a full burner of twice the heat release rate [17,18]. So, taking this method, the critical velocity of near-wall fire should be equal to the case of a fire with twice the heat release rate in a tunnel with twice the cross sectional area. However, even in this way, the model of Thomas, Oka, Wu and Danziger still cannot account for the condition of near-wall fire, due to its rough physical model by considering the overall energy balance. That is, the value of Q^* in these models does not vary under the near-wall condition even with "mirror" effect considered. Based on the model of Kunsch, as the value of $\Delta T_0{}^* Q''^{2/3}$ is usually much smaller than 1, it can be approximated that

$$U_c \propto Q^{1/3} \tag{11}$$

This is in accordance with the report of parametric study by Vauquelin [12]. So, it can be approximately anticipated that

$$U_{c,w}/U_{c,c} = (2Q/Q)^{1/3} = 1.26 \tag{12}$$

However, it should be noted that the above value is an ideal one. The "mirror" effect of near-wall plume in compartment fires is basically applied when the area of the fire source is relatively very small to that of the floor, or in a semi-infinite boundary condition, to consider the effect of the wall only. In a confinement space as the tunnel, the width or the cross sectional area is in a limited value. There should also be an interaction of fire plume with the longitudinal flow, which was largely influenced by the tunnel cross sectional size and the fire size.

4. CFD modelling

4.1. The turbulent airflow model

CFD modelling is now widely used in fire safety engineering to simulate buoyancy induced flow [19–21]. Turbulence models commonly used in CFD are based on Reynolds averaging Navier Stokes equation (RANS) method, large eddy simulation (LES) and direct numerical simulation (DNS). LES turbulent model, which is now more widely used and reported to give better predictions on some cases [22] of buoyancy driven flow, was used in this paper.

In LES modelling, the turbulence motion with scale larger than the grid size is computed directly while the one less than the grid size is modelled by SGM model. Thus, two points should be considered [20,22]:

- fine enough grids; and
- a suitable sub-grid model (SGM) on small eddies.

The grid size should be fine enough to include the turbulence scales associated with the largest eddy motions which can be described accurately enough by the SGM. The LES sub-grid model commonly used in LES was developed originally by Smagorinsky [23].

The CFD software, fire dynamics simulator (FDS), was used for simulation in this paper with a recent version of 4.07, which was released on March 10, 2006 by the national institute of standards and technology (NIST) [24,25]. A refined filtered dynamics sub-grid model is applied in the FDS model to account for the sub-grid scale motion of viscosity, thermal conductivity and material diffusivity [25]. The dynamic viscosity defined in FDS is

$$\mu_{ijk} = \rho_{ijk}(C_S\Delta)^2|S| \tag{13}$$

where C_S is an empirical Smagorinsky constant, Δ is $(\delta x \delta y \delta z)^{1/3}$ and

$$|S| = 2\left(\frac{\partial u}{\partial x}\right)^2 + 2\left(\frac{\partial v}{\partial y}\right)^2 + 2\left(\frac{\partial w}{\partial z}\right)^2 + \left(\frac{\partial u}{\partial x} + \frac{\partial v}{\partial y}\right)^2 + \left(\frac{\partial u}{\partial z} + \frac{\partial w}{\partial x}\right)^2 + \left(\frac{\partial v}{\partial z} + \frac{\partial w}{\partial y}\right)^2 - \frac{2}{3}(\nabla \cdot \vec{u})^2 \quad (14)$$

The term $|S|$ consists of second-order spatial differences averaged at the grid centre. The thermal conductivity k_{ijk} and material diffusivity D_{ijk} of the fluid are related to the viscosity μ_{ijk} in terms of the Prandtl number Pr and Schmidt number Sc by

$$k_{ijk} = \frac{c_p \mu_{ijk}}{Pr}; \quad (\rho D)_{ijk} = \frac{\mu_{ijk}}{Sc} \quad (15)$$

Both Pr and Sc are assumed to be constant. The specific heat c_p is taken to be that of the dominant species of the mixture [25].

In the Smagorinsky sub-grid model, the constant C_S is an important but sensitive parameter. It is flow dependent and has been optimized over a range from 0.1 to 0.25 for various flow fields. Zhang et al. [19] had studied the effect of the Smagorinsky sub-grid scale model coefficients, C_S and Pr, on predicted turbulence statistical quantities in a fire room. Two values of C_S, 0.14 and 0.18, and two values of Pr, 0.2 and 0.9, were tested. Results showed that for a strong buoyant plume, the predictions of the mean velocity and temperature and also the turbulent statistical quantities using C_S of 0.18 are much better than C_S of 0.14. Comparisons also indicated that setting the Pr to be 0.2 should be more reasonable for simulating the room fire. It was also reported that taking C_S as 0.2 gave good predictions for buoyancy-driven flow [26] and a channel flow [27] with fine enough grid resolution. According to these validation works, the constants C_S, Pr and Sc are defaulted in FDS as 0.2, 0.2 and 0.5, respectively. It was reported that for some cases in simulating buoyancy-drive flow [26], the predicted values from the filtered dynamics sub-grid model by FDS agreed better with the measured value than those from the original Smagorinsky model and RANS.

In FDS, thermal radiation is computed by the radiative transfer equation (RTE), which is solved by using finite volume method (FVM) [25]. In order to consider the spectral dependence, the radiation spectrum is divided into a relatively small number of narrow bands, and a separate RTE is derived for each band. The RTE was simplified as follows:

$$s\nabla I_n(x, s) = \kappa_n(x, \lambda)[I_{b,n}(x) - I_n(x, s)], \quad n = 1 \ldots N \quad (16)$$

The Courant-Friedrichs-Lewy (CFL) criterion [28,29] is used in FDS [25] for justifying convergence. This criterion is more important for large-scale calculations where convective transport dominates the diffusive one. In FDS, the estimated velocities are tested at each time step to ensure that the CFL condition is satisfied [25]:

$$\delta t \max\left(\frac{|u_{ijk}|}{\delta x}, \frac{|v_{ijk}|}{\delta y}, \frac{|w_{ijk}|}{\delta z}\right) < 1 \quad (17)$$

The initial time step is set automatically in FDS by the size of a grid cell divided by the characteristic velocity of the flow. The default value of the initial time step is $\frac{5(\delta x \delta y \delta z)^{1/3}}{\sqrt{gH}}$, where δx, δy, and δz are the dimensions of the smallest grid cell, H is the height of the computational domain and g is the acceleration due to gravity [25]. During the calculation, the time step is varying and constrained by the convective and diffusive transport speeds to ensure that the CFL condition is satisfied at each time step [25]. The time step will eventually change to a quasi-steady value when the fire environment reached a quasi-steady state.

The FDS model had been successfully applied to study the fire-induced transportation of smoke and carbon monoxide in a long channel [5], dispersion of propane under a leakage condition in a room [30] and contamination levels in near and far field in a warehouse facility under forced ventilation [31].

4.2. The physical model

CFD simulation was performed for a road tunnel model with length of 50 m and a full scale cross section of width of 10 m and height of 7.2 m as shown in Fig. 2. The cross section in this size is commonly seen in China for double tube road tunnel with two lanes in each tube. The two ends of the tunnel were both set to be naturally opened with no initial velocity boundary condition specified for these openings. The longitudinal wind velocity was set by the "MISC" command provided by FDS [24], which can directly prescribe an initial wind through the domain. By this method, a steady uniform longitudinal wind was initialized at the beginning of the simulation. Four types of thermal boundary conditions can be used in FDS [24]:

- fixed temperature solid surface;
- fixed heat flux solid surface;
- thermally-thick solid; or
- thermally-thin sheet.

Fixed temperature or fixed heat flux boundary conditions are only of limited usefulness in real fire scenarios [24]. Thermally-thick boundary condition was selected. That is, the tunnel wall heats up due to radiative and convective heat transfer from the surrounding gas, by specifying the thermal conductivity, density, specific heat and the thickness of the material. The internal lining of the tunnel was specified as "CONCRETE". The thermal properties of this material are available in the FDS database documentation.

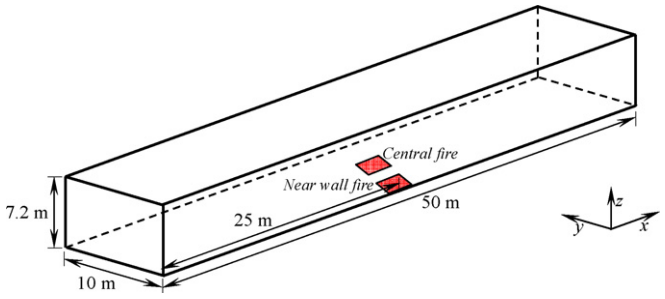

Fig. 2. Physical model for CFD modelling.

In applying LES simulation, the grid size is a key parameter to be considered carefully first. A grid sensitivity and model verification studies had been formerly performed [32] with the same sized physical tunnel fire model. Grid system with the grid size of 0.083 m in the near fire region and of 0.167 m for the other region was finally used. The smoke temperatures below the tunnel ceiling at 3 and 20 m upstream from the fire predicted by this grid system were compared with measured values from full-scale tests [34] in Fig. 3. It was shown that the smoke flow temperatures predicted were in good agreement with full-scale experimental data. This kind of grid system was also used in CFD modelling of this paper.

The fire source was placed at the centre of the domain, freely standing or near the sidewall. Square pool fires were used. The heat outputs were determined by fire source area size and heat release rate per unit area (HRRPUA) as provided in FDS. A mixture fraction-based combustion model is used in the LES simulation of FDS. A reaction type of "CRUDE OIL" according to FDS reaction database [5,24] was also specified for generating smoke from the fire source and this does not influence the heat output of the fire. In order to consider purely the effect of the sidewall confinement, the relative fire source width is to be considered. It should not be too large compared with the width of the tunnel. So, the fire sizes considered

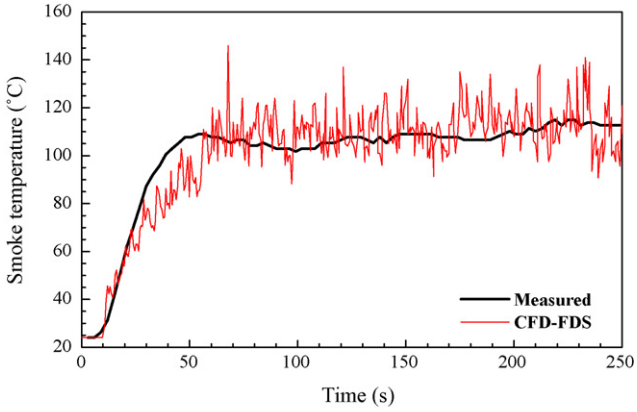

(a) at 3 m upstream from the fire

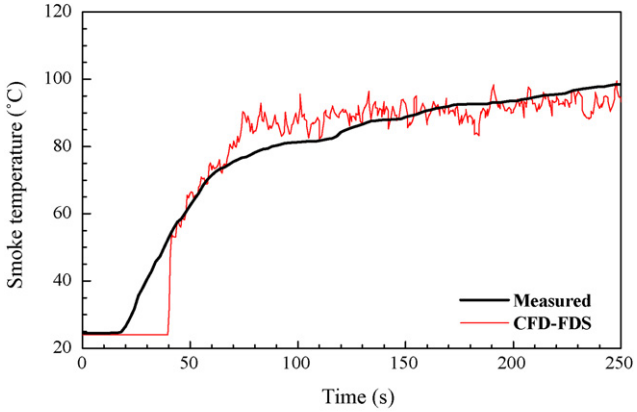

(b) at 20 m upstream from the fire

Fig. 3. Model verification by comparison of smoke temperature predicted by FDS with measure data in full scale tests.

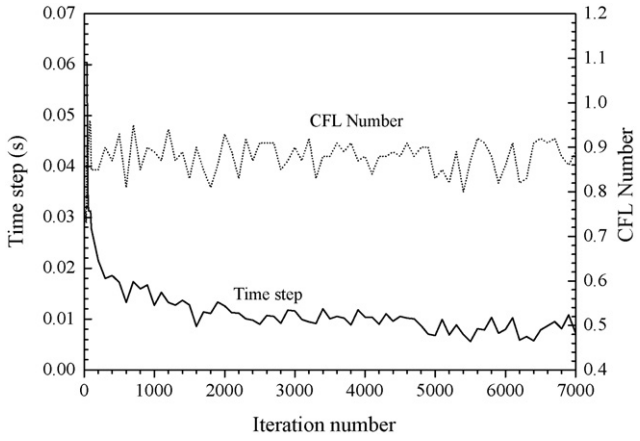

Fig. 4. Convergence and time steps during simulation.

were 0.5, 1, 1.5, 2, 3, 4, 6, 8, 12 and 16 MW with HRRPUA of 1 MW m^{-2}.

All simulations were run in a personal computer with 3.0 G CPU and 4 GB RAM. The CFL numbers during the iterations were in the range of 0.72–0.96, all less than the criteria value of 1. The CFL number and the time steps during the simulation are shown in Fig. 4. The CFL convergence condition was satisfied.

5. Results and discussion

5.1. The fire plume

The typical instantaneous temperature fields of the plume, for example 1 MW fire, at the quasi-stable condition when the upwind gas dispersion was arrested by the wind, are compared between central freely standing fire and near-wall fire in Fig. 5. Firstly, it can be seen that when the fire positioned near the sidewall, the width, or the radius, of the fire plume was smaller than that of central fire. This indicated that more fresh air was entrained into the plume of a central freely standing fire rather than near the sidewall, as anticipated before. Lower entrainment of fresh air resulted in higher plume temperature at the impingement region on the ceiling. For the fire of 1 MW and 1.4 m s^{-1} longitudinal wind speed, it was only 60 °C for the central freely standing fire, but up to 80 °C for the near-wall fire. Under the longitudinal wind speed of 1.4 m s^{-1}, the upstream hot gas flow was arrested as it did not travel beyond the fire source in a freely standing fire condition, but clearly beyond the fire source in a near-wall fire. Till the longitudinal wind speed was increased to 1.6 m s^{-1}, the upwind hot gas flow was arrested for the near-wall fire.

The quasi-stable state for the development of the plume and the dispersion of smoke particles beneath the tunnel ceiling are also shown in Fig. 6. It can also be clearly seen that the fire plume width in a freely standing condition was larger than in a near-wall condition. The upwind smoke flow was arrested by 1.4 m s^{-1} wind for freely standing fire and by up to 1.6 m s^{-1} wind for near-wall fire.

So, it was clearly shown that larger critical velocity was needed to arrest the upwind gas and smoke dispersion for near-

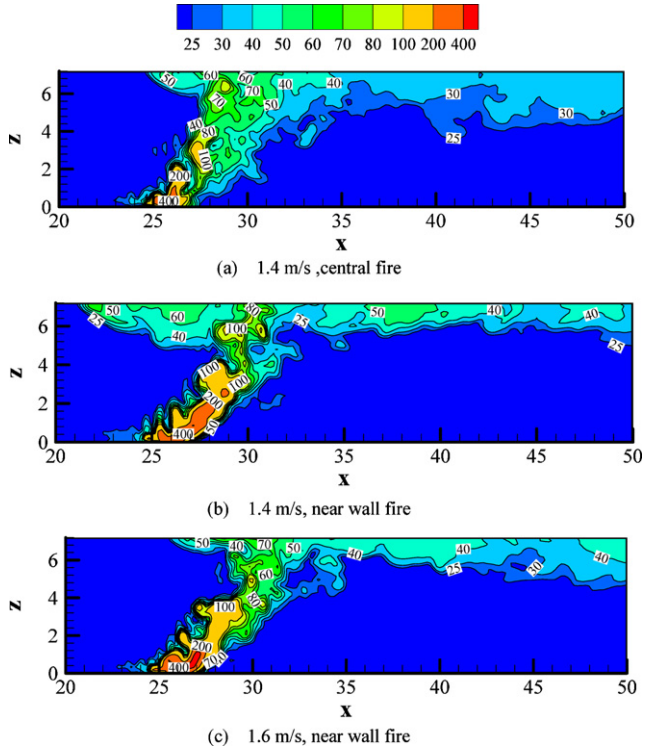

Fig. 5. Temperature field of fire plume for near wall fire and central fire.

wall fire. For the fire of 1 MW, the critical velocity was 1.4 m s^{-1}. But the wind of this speed certainly cannot arrest the same fire positioned near the sidewall as shown in Fig. 1. The critical velocity of this fire near the wall was up to 1.6 m s^{-1}.

5.2. Critical velocity

The critical velocity for arresting the upwind gas and smoke dispersion predicted by CFD simulation for both near-wall fire and freely standing central fire are compared with former models by Thomas, Danziger, Oka, Wu and Kunsch in Fig. 7. A series of full-scale experiments had also been conducted in operating highway road tunnels, as a part of a long-term tunnel fire research program in China. The objectives are to have a better understanding of the fire dynamics and smoke control in tunnel fires. Among these full scale experiments, the upstream distances of the fire gas and smoke dispersion under different longitudinal wind velocities and thus, the critical velocities for arresting the upwind gas and smoke dispersion for 1.8 and 3.2 MW pool fire were measured. The fire was positioned at the centre of the tunnel. The fire near the wall was not tested as it would damage the tunnel wall. The tunnel was 10.8 m wide and 7.2 m high. More detailed information on these full-scale tunnel fire tests can be found in the former reports [33–35]. The critical velocities were measured to be 1.75 and 2.0 m s^{-1} for the two fires. These two values are also shown in Fig. 7.

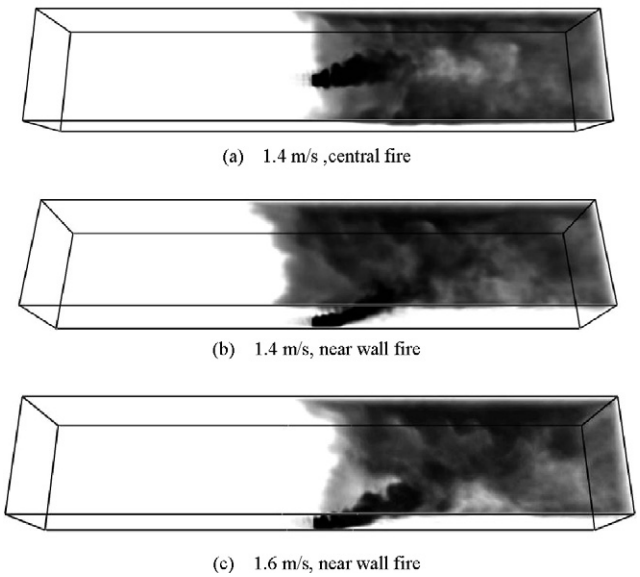

Fig. 6. Dispersion of smoke particles beneath the ceiling for near wall fire and central fire.

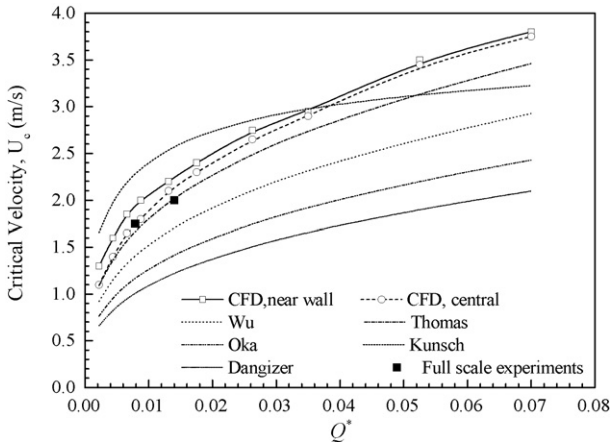

Fig. 7. Comparison of critical velocity predicted by CFD modelling with that by former models.

It can be seen that the increase trend of critical velocity with fire size predicted by the CFD modelling was similar to the model of Thomas, Danziger, Oka and Wu. However, the predictions by these models seemed to be all lower than those of the full scale CFD modelling. The predictions made by the model of Thomas seemed to be closest to those of the CFD modelling. Their predictions at lower fire sizes were very near and both close to the two full scales experimental measured data. The increase of critical velocity with fire size predicted by Kunsch's model seemed to be in different trend with others. The predictions made by Kunsch's model was larger than those of the CFD modelling when Q^* was less than 0.035, and smaller when Q^* was larger than 0.035. It was also shown in Fig. 7 that the critical velocity of a near-wall fire was larger than those of same fire freely standing at the tunnel centre. However, with the increase of the fire size, their difference will decreased so that these two curves seemed to be closer.

The ratio of critical velocity of near-wall fire to that of the freely standing central fire, $U_{c,w}/U_{c,c}$, was plotted against dimensionless fire heat release rate, Q^*, in Fig. 8. It was clearly shown that with the increase of the fire size, the ratio of $U_{c,w}/U_{c,c}$ decreases to become more and more nearer to unity. This indi-

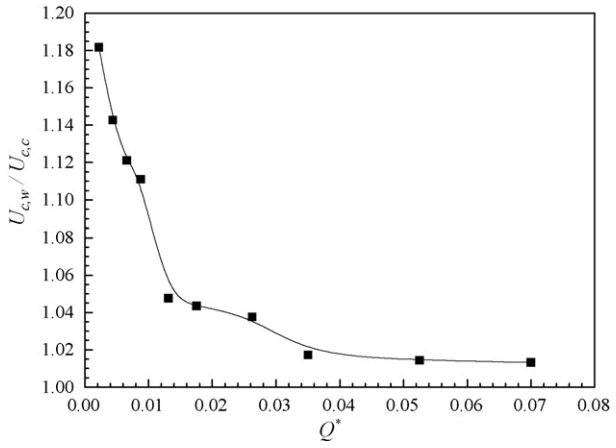

Fig. 8. Ratio of critical velocity for near wall fire to that for central fire vs. dimensionless HRR.

cated that the sidewall effect on the critical velocity was clearer for small-sized fire than for large fire. As larger fire with higher heat release should have bigger area and width, with the increase of the fire heat release rate, the fire source width will be nearer to the tunnel width and the fire situation of a near-wall fire will be nearer to a central fire. It can be anticipated that when the fire source area or width was near or equal to the width of the tunnel, there should be no difference between a "freely standing central fire" and a "near-wall fire" anymore. They are both "near-wall fire" and the ratio should be equal to unity under this situation.

It can be also seen that the ratio of $U_{c,w}/U_{c,c}$ by CFD simulation was closest to the theoretical estimated value for lowest non-dimensional heat release rate. It was about 1.18 for the 500 kW fire. This was near to the ideal value of 1.26 estimated before. This is due to the basic assumption of the "mirror" effect theory. That is, the area of the fire source should be relatively very small to that of the floor. In a confinement space as the tunnel, the width or the cross sectional area is in a limited value. There should also be an interaction of fire plume with the longitudinal flow, which is largely influenced by the tunnel cross sectional size and the fire size. In case of relative small fire in a tunnel, the real situation is more like the basic assumption of "mirror" effect. That is why the ratio with lowest non-dimensional heat release rate was closest to the theory. However, the ideally estimated value was still a bit higher than the value obtained by the CFD modeling even for the very small fire. It should be due to the fact that the cold sidewall cools the fire plume. This resulted in the decrease of the plume temperature and thus the buoyancy force of the upwind gas flow, with less critical velocity to arrest it.

6. Conclusions

This paper studied the critical wind velocity for arresting upwind gas and smoke dispersion induced by fire near the sidewall in road tunnels, as a different but more realistic fire situation than arbitrarily assuming that the fire originates at the tunnel centre in all former models. Results showed that when fire originates near the wall, it needs larger critical velocity to arrest the upwind transportation of the hot gas and the smoke particle. This is an important issue to be considered by the safety manager for designing the longitudinal ventilation system for tunnels.

Ideally, the ratio of critical velocity of near wall fire to that of freely standing central fire was theoretically estimated to be 1.26. Results by CFD modelling showed that the ratio was decreased with the increase of the fire size till close to unity. The ratio by CFD modelling was about 1.18 for a 500 kW small fire, being near to and a bit lower than the theoretically estimated value of 1.26. The variation of the ratio of critical velocity of near-wall fire to that of central fire, with fire size, was finally provided for reference.

Acknowledgements

This work was supported by Anhui Provincial Natural Science Foundation under Grant No. 070415224 and China Postdoctoral Science Foundation under Grant No. 20060400203.

References

[1] F. Vuilleumier, A. Weatherill, B. Crausaz, Safety aspects of railway and road tunnel: example of the Lotschberg railway tunnel and Mont-Blanc road tunnel, Tunn. Undergr. Sp. Technol. 17 (2002) 153–158.
[2] A. Leitner, The fire catastrophe in the Tauern Tunnel: experience and conclusions for the Austrian Guidelines, Tunn. Undergr. Sp. Technol. 16 (2001) 217–223.
[3] W.H. Hong, The progress and controlling situation of Daegu subway fire disaster, in: 6th Asia-Oceania Symposium on Fire Science and Technology, 17–20 March, 2004, Daegu, Korea, 2004, pp. 28–46.
[4] SCMP, Fire engulfs Alpine Tunnel, killing two, South China Morning Post (SCMP), International, 2005, p. A15, 6 June.
[5] L.H. Hu, N.K. Fong, L.Z. Yang, W.K. Chow, Y.Z. Li, R. Huo, Modeling fire-induced smoke spread and carbon monoxide transportation in a long channel: fire dynamics simulator comparisons with measured data, J. Hazard. Mater. 140 (2007) 293–298.
[6] N.H. Danziger, W.D. Kennedy, Longitudinal ventilation analysis for the Glenwood canyon tunnels, in: Proceedings of the Fourth International Symposium Aerodynamics and Ventilation of Vehicle Tunnels, 1982, pp. 169–186.
[7] Y. Oka, G.T. Atkinson, Control of smoke flow in tunnel fires, Fire Safety J. 25 (1995) 305–322.
[8] G.B. Grant, S.F. Jagger, C.J. Lea, Fires in tunnels, Phil. Trans. R. Soc. Theme Issue on Fire Dynamics 356 (1998) 2873–2906.
[9] G.B. Grant, S.F. Jagger, Use of tunnel ventilation for fire safety, in: The Handbook of Tunnel Fire Safety, Thomas Telford, Ltd, 2005.
[10] J.P. Kunsch, Critical velocity and range of a fire-gas plume in a ventilated tunnel, Atmos. Environ. 33 (1999) 13–24.
[11] J.P. Kunsch, Simple model for control of fire gases in a ventilated tunnel, Fire Safety J. 37 (2002) 67–81.
[12] O. Vauquelin, Parametrical study of the back flow occurrence in case of a buoyant release into a rectangular channel, Exp. Therm. Fluid Sci. 29 (2005) 725–731.
[13] P.H. Thomas, The Movement of Buoyant Fluid Against a Stream and the Venting of Underground Fires, Fire Research Note No. 351, Fire Research Station, Watford, UK, 1958.
[14] P.H. Thomas, The Movement of Smoke in Horizontal Passages Against an Air Flow, Fire Research Note, No. 723, Fire Research Station, Watford, UK, 1968.
[15] C.K. Lee, R.F. Chaiken, J.M. Singer, Interaction between duct fires and ventilation flow: an experimental study, Combust. Sci. Technol. 20 (1979) 59–72.
[16] Y. Wu, M.Z.A. Bakar, Control of smoke flow in tunnel fires using longitudinal ventilation systems- a study of the critical velocity, Fire Safety J. 35 (2000) 363–390.

[17] L.H. Hu, Y.Z. Li, R. Huo, L. Yi, C.L. Shi, W.K. Chow, Experimental studies on the rise time of buoyant fire plume fronts induced by pool fires, J. Fire Sci. 22 (1) (2004) 69–86.
[18] B. Karlsson, J.G. Quintiere, Fire plumes and flame heights, in: Enclosure Fire Dynamics, CRC Press LLC, 2000 N.W. Corporate Blvd, Boca Raton, Florida, 1999, p. 33431 (Chapter 4).
[19] W. Zhang, A. Hamer, M. Klassen, D. Carpenter, R. Roby, Turbulence statistics in a fire room model by large eddy simulation, Fire Safety J. 37 (2002) 721–752.
[20] G. Cox, S. Kumar, Modeling enclosure fires using CFD, in: The SFPE Handbook of Fire Protection Engineering, third ed., National Fire Protection Association, Inc, Auincy, Massachusetts, 2002 (Chapter 8).
[21] Y.F. Li, W.K. Chow, Computational fluid dynamics simulation of fire-induced air flow in a large space building: key points to note, in: Proceedings of the ASME Heat Transfer/Fluids Engineering Summer Conference HT/FED, 2004, pp. 1163–1169.
[22] Y. Jiang, Q.Y. Chen, Buoyancy-driven single-sided natural ventilation in building with large openings, Int. J. Heat Mass Transfer 46 (2003) 973–988.
[23] J. Smagorinsky, General circulation experiments with primitive equations-I, the basic experiment, Mon. Weather Rev. 91 (1963) 99–105.
[24] K. McGrattan, G. Forney, Fire Dynamics Simulator (Version 4.07) User's Guide, National Institute of Standards and Technology, 2006.
[25] K. McGrattan, Fire Dynamics Simulator (Version 4.07) Technical Reference Guide, National Institute of Standards and Technology, 2006.
[26] Y. Jiang, Q. Chen, Buoyancy-driven single-sided natural ventilation in building with large openings, Int. J. Heat Mass Transfer 46 (2003) 973–988.
[27] P.J. Mason, N.S. Callen, On the magnitude of the subgrid-scale eddy coefficient in large-eddy simulations of turbulent channel flow, J. Fluid Mech. 162 (1986) 439–462.
[28] R. Courant, K. Friedrichs, H. Lewy, On partial difference equations of mathematical physics, IBM J. Res. Dev. 11 (1967) 215–234 (English translation of the original work in Math. Ann. Vol.100, 1928, pp. 32–74).
[29] W. Zhang, N. Ryder, R.J. Roby, D. Carpenter, Modeling of the combustion in compartment fires using large eddy simulation approach, in: Proceedings of the 2001 Fall Technical Meeting, Eastern States Section, December, Combustion Institute, Pittsburgh, Pennsylvania, 2001.
[30] N.L. Ryder, J.A. Sutula, C.F. Schemel, A.J. Hamer, V.V. Brunt, Consequence modeling using the fire dynamics simulator, J. Hazard. Mater. 115 (2004) 149–154.
[31] N.L. Ryder, C.F. Schemel, S.P. Jankiewicz, Near and far field contamination modeling in a large-scale enclosure: fire dynamics simulator comparisons with measured observations, J. Hazard. Mater. 130 (2006) 182–186.
[32] Hu, L.H., Chow, W.K., Huo, R., Studies on buoyancy-driven back-layering in tunnel fires, Experimental Thermal and Fluid Science (revised, 2006).
[33] L.H. Hu, R. Huo, W. Peng, W.K. Chow, R.X. Yang, On the maximum smoke temperature under ceiling in tunnel fires, Tunn. Undergr. Sp. Technol. 21 (2006) 650–655.
[34] Hu, L.H., Huo, R., Wang, H.B., Li, Y.Z., Yang, R.X., 2006, Experimental studies on fire-induced buoyant smoke temperature distribution along tunnel ceiling, Building and Environment, in press.
[35] L.H. Hu, R. Huo, H.B. Wang, R.X. Yang, Experimental and numerical studies on longitudinal smoke temperature distribution upstream and downstream from the fire in a road tunnel, J. Fire Sci. 25 (1) (2007) 23–43.